CHINESE JOURNAL OF MECHANICAL ENGINEERING
Vol. 26, No. 5, 2013

DOI: 10.3901/CJME.2013.05.1022, available online at www.springerlink.com; www.cjmenet.com; www.cjmenet.com.cn

Flexible Time Domain Averaging Technique

ZHAO Ming[1], LIN Jing[2, 3, *], LEI Yaguo[1, 3], and WANG Xiufeng[1, 3]

1 *School of Mechanical Engineering, Xi'an Jiaotong University, Xi'an 710049, China*
2 *State Key Laboratory for Manufacturing Systems Engineering, Xi'an Jiaotong University, Xi'an 710054, China*
3 *Shaanxi Key Laboratory of Product Quality Assurance & Diagnosis, Xi'an 710054, China*

Received September 26, 2012; revised June 1, 2013; accepted June 14, 2013

Abstract: Time domain averaging(TDA) is essentially a comb filter, it cannot extract the specified harmonics which may be caused by some faults, such as gear eccentric. Meanwhile, TDA always suffers from period cutting error(PCE) to different extent. Several improved TDA methods have been proposed, however they cannot completely eliminate the waveform reconstruction error caused by PCE. In order to overcome the shortcomings of conventional methods, a flexible time domain averaging(FTDA) technique is established, which adapts to the analyzed signal through adjusting each harmonic of the comb filter. In this technique, the explicit form of FTDA is first constructed by frequency domain sampling. Subsequently, chirp Z-transform(CZT) is employed in the algorithm of FTDA, which can improve the calculating efficiency significantly. Since the signal is reconstructed in the continuous time domain, there is no PCE in the FTDA. To validate the effectiveness of FTDA in the signal de-noising, interpolation and harmonic reconstruction, a simulated multi-components periodic signal that corrupted by noise is processed by FTDA. The simulation results show that the FTDA is capable of recovering the periodic components from the background noise effectively. Moreover, it can improve the signal-to-noise ratio by 7.9 dB compared with conventional ones. Experiments are also carried out on gearbox test rigs with chipped tooth and eccentricity gear, respectively. It is shown that the FTDA can identify the direction and severity of the eccentricity gear, and further enhances the amplitudes of impulses by 35%. The proposed technique not only solves the problem of PCE, but also provides a useful tool for the fault symptom extraction of rotating machinery.

Key words: time domain averaging, chirp Z-transform, period cutting error, de-noising, interpolation

1 Introduction

Rotating machines play an important role in the morden industry and their failure may lead to fatal accidents and economical loss. Therefore, the fault detection of rotating machinery has received considerable attention during the past decades. Various condition monitoring techniques have been developed up to now[1–2]. Among those, vibration analysis has been extensively studied, and proven to be effective in the fault detection[3–6].

Time domain averaging(TDA) is a classic technique to extract periodic components from noisy vibration signals[7–8]. It has been used widely to analyze vibration signals from rotating machine components, such as gears and rolling element bearings[9–11]. Traditionally, TDA is implemented by dividing a time-domain waveform into segments in terms of the signal period we concern, and then averaging the corresponding data among all segments. In this procedure, the synchronous components remain unchanged, whereas the asynchronous components and noise signals are suppressed, the signal-to-noise ratio(SNR) is enhanced thereafter[12–14]. Although TDA has been proven to be effective in vibration analysis, there are still some limitations associated with TDA.

Firstly, the prerequisite of conventional TDA is that the signal should be exactly divisible by its period, otherwise, the effectiveness will be affected greatly due to period cutting error[15]. However, this condition cannot be satisfied in many practical applications since the sampling frequency is not necessarily an exact integer multiple of rotating frequency of the machinery. Several methods have been developed to solve this issue. MCFADDEN[16] introduced an off-line interpolation method to reduce period cutting error by utilizing a reference signal. Unfortunately, higher order interpolation is required in order to achieve a flatter frequency response in the pass-band, which is time consuming to some extent. LIU, et al[15], proposed an improved algorithm which can limit the period cutting error less than half a sampling interval. However, the number of averaging period should be carefully chosen in this method, otherwise, the performance will be degraded significantly. WU, et al[17], improved the performance of TDA by employing a fractional delay filter to eliminate period

* Corresponding author. E-mail: jinglin@mail.xjtu.edu.cn
This project is supported by National Natural Science Foundation of China(Grant Nos. 51125022, 51005173), PhD Programs Foundation of Ministry of Education of China(Grant No. 20110201110025), and the Fundamental Research Funds for the Central Universities of China
© Chinese Mechanical Engineering Society and Springer-Verlag Berlin Heidelberg 2013

cutting error, which needs to design an all-pass FIR filter and always suffers from boundary effect. Recently, BRAUN[18] reviewed the TDA method from the view of comb filter and proposed some approaches that are less sensitive to the period cutting error, but those algorithms cannot eliminate it completely.

Secondly, as a comb filter, the output waveform of the conventional TDA contains total contribution of fundamental frequency and its all harmonics. However, in many practical applications, we are only interested in the waveform corresponding to some specified harmonics. For instance, in the gear eccentricity detection[19], we need to determine the waveform corresponding to the first-order sidebands around the meshing frequency so as to identify the direction and severity of the eccentric gear. In the residual signal analysis[20–21], the meshing component should be removed from the signal in order to highlight the changes caused by gear fault. Those requirements are frequently encountered in fault diagnosis of rotating machinery.

To overcome those limitations of conventional TDA, a new technique named flexible TDA(FTDA) is proposed in this paper. It is implemented by using chirp Z-transform. Essentially, there is no period cutting error in this technique. Furthermore, it can provide a flexible waveform output in time-domain to satisfy different requirements, such as harmonic extraction, filtering or interpolation.

The rest of this paper is organized as follows. Conventional TDA is reviewed in section 2. The relationship between continuous TDA algorithm and frequency domain sampling is investigated at the beginning of section 3. The algorithm of FTDA is proposed subsequently. The efficiency of FTDA is demonstrated by simulations and experiments in sections 4 and 5, respectively. Finally, some conclusions are given in section 6.

2 Review of Time Domain Averaging Method

Generally, the vibration signals measured from rotating machinery are a combination of periodic signals and interferences, which can be written as

$$x(t) = s(t) + w(t), \tag{1}$$

where $s(t)$ is the periodic signal with period T_0 (the fundamental frequency is $f_0 = 1/T_0$ accordingly), $w(t)$ denotes the measurement noise and other asynchronous components. In TDA, the vibration signal $x(t)$ is divided into segments according to the exact period of T_0, then all the segments are added together for averaging. In this procedure, the noise and asynchronous components are attenuated, while the periodic components are remained thereafter. The procedure can be formulated as

$$y(t) = \frac{1}{N}\sum_{r=0}^{N-1} x(t + rT_0). \tag{2}$$

We refer to Eq. (2) as continuous TDA (CTDA), since the output of which is a function of continuous variable t. There is no period cutting error in CTDA because $x(t)$ can be separated exactly according to the period T_0 in the continuous time domain. However, things are different when $x(t)$ is discretized.

Suppose $x(t)$ is sampled with a sampling interval Δt, then Eq. (1) becomes

$$x(n\Delta t) = s(n\Delta t) + w(n\Delta t). \tag{3}$$

As a consequence, the corresponding discrete TDA, abbreviated as TDA, can be given as

$$y(n\Delta t) = \frac{1}{N}\sum_{r=0}^{N-1} x\left(n\Delta t + rM\Delta t\right), \tag{4}$$

where M is the number of samples per period. In practice, M is usually determined by $M = [T_0/\Delta t]$, and $[\cdot]$ denotes the rounding function for the nearest integer. The transfer function of Eq. (4) is given by

$$|H(f)| = \frac{1}{N}\left|\frac{\sin\left(\pi N f/f_{\mathrm{p}}\right)}{\sin\left(\pi f/f_{\mathrm{p}}\right)}\right|,\ f_{\mathrm{p}} = \frac{1}{M\Delta t}. \tag{5}$$

The frequency response of Eq. (5) looks like a comb, which is illustrated in Fig. 1. The position of each tooth is at the integer multiple of f_{p}. The performance of TDA is highly depended on the relationship between f_{p} and f_0. When the fundamental period T_0 is an exact integral multiple of the sampling interval Δt, (or equivalently, the sampling frequency f_{s} is an exact integral multiple of f_0), it immediately follows that $f_{\mathrm{p}} = f_0$. In this case, TDA works well since all the synchronous components with period T_0 are reserved, whereas the interferences are suppressed as illustrated in Fig. 1. However, for a variety of practical applications, we cannot guarantee that f_{s} is an exact integral multiple of f_0. In those cases, the comb teeth will not locate at the multiples of f_0 any more, which implies that the synchronous components will be suppressed at same time. The attenuation coefficient for the kth synchronous component, denoted by C_k, can be obtained by replacing f with kf_0 in Eq. (5), which yields

$$C_k = \frac{1}{N}\left|\frac{\sin\left(\pi N k f_0/f_{\mathrm{p}}\right)}{\sin\left(\pi k f_0/f_{\mathrm{p}}\right)}\right|. \tag{6}$$

Taking $f_{\mathrm{p}} = 1.01 f_0$ for example, the evolution of C_k with N is illustrated in Fig. 2. It is noticed that the attenuation effect tends to aggravate with the increment of N. That

explains why conventional TDA fails to work when period cutting error exists.

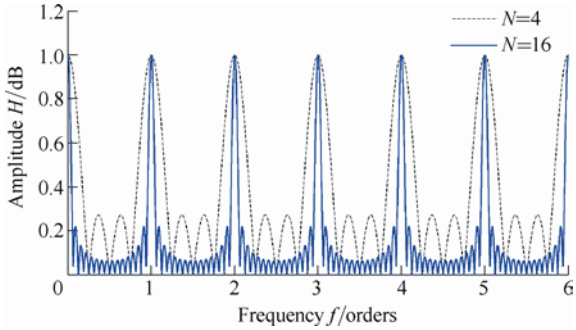

Fig. 1.　Frequency response of TDA

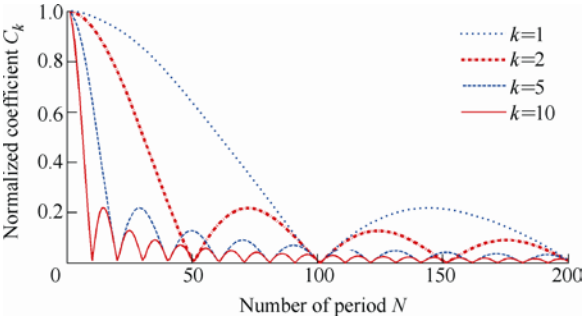

Fig. 2.　Relationship between C_k and N

3　Flexible TDA Algorithm

As discussed in the previous section, the performance of conventional TDA is affected by the period cutting error, which always comes from the discretization of signal. Therefore, the relationship between CTDA and frequency domain sampling is first investigated in this section. Then, the FTDA algorithm for original data $x[n]$ is proposed. Finally, how to perform de-noising, harmonics extraction, interpolation and filtering by using FTDA is discussed.

3.1　CTDA and frequency domain sampling

Theoretically, the noise corrupted periodic signal $x_a(t)$ is always defined on the whole time axis. However, this definition is a little impractical in application, since the real data is always measured within a limited time interval. Therefore, the analyzed signal in CTDA is a truncation form of $x_a(t)$, which is given by

$$x(t)=x_a(t)w(t)\,, \tag{7}$$

where T_0 is the fundamental period, $w(t)$ is a rectangular window function with time duration of NT_0.

The spectrum of $x(t)$ is given by

$$X(\omega)=\int_0^{NT_0}x(t)\exp(-\mathrm{j}\omega t)\mathrm{d}t\,. \tag{8}$$

According to the sampling theorem, sampling in time domain corresponds to periodic extension in frequency domain, and frequency aliasing will not happen as long as the sampling frequency is greater than twice of the highest frequency of the signal. On the other hand, sampling in frequency domain also corresponds to periodic extension in time domain. Aliasing is a phenomenon that we try to avoid in many applications. However, in this paper, we will utilize aliasing effect, so as to produce the overlapping and averaging in the time domain, which is exactly we need in CTDA. In order to achieve that purpose, we construct the frequency domain sampling function as follows:

$$S(\omega)=\frac{\omega_0}{N}\sum_{n=-\infty}^{\infty}\delta(\omega+n\omega_0)\,, \tag{9}$$

where $\omega_0=2\pi/T_0$ is the sampling interval in frequency domain. The sampled signal of $X(\omega)$ can be represented as

$$X_{\mathrm{p}}(\omega)=X(\omega)\bullet S(\omega)=\frac{\omega_0}{N}\sum_{n=-\infty}^{\infty}X(-n\omega_0)\bullet\delta(\omega+n\omega_0)\,, \tag{10}$$

According to convolution theorem, the time domain signal $\tilde{x}(t)$ corresponding to $X_{\mathrm{p}}(\omega)$ can be obtained by

$$\tilde{x}(t)=F^{-1}\left[X(\omega)\right]*F^{-1}\left[\frac{\omega_0}{N}\sum_{n=-\infty}^{\infty}\delta(\omega+n\omega_0)\right]=$$
$$x(t)*\frac{1}{N}\sum_{n=-\infty}^{\infty}\delta(t+nT_0)=\frac{1}{N}\sum_{n=-\infty}^{\infty}x(t+nT_0), \tag{11}$$

where * denotes the convolution operation and F^{-1} stands for the inverse Fourier transform.

Obviously, $\tilde{x}(t)$ has a period of T_0. In order to obtain the relationship between $\tilde{x}(t)$ and CTDA, we examine $\tilde{x}(t)$ within one period, e.g. $[0,T_0]$. Then, Eq. (11) can be simplified as Eq. (12), since $x(t)$ is zero outside $[0,NT_0]$:

$$\tilde{x}(t)=\frac{1}{N}\sum_{n=0}^{N-1}x(t+nT_0),\quad t\in[0,T_0]. \tag{12}$$

By comparison of Eq. (12) and Eq. (2), it is obvious that $\tilde{x}(t)$ is exactly the periodic extension of CTDA.

On the other hand, $\tilde{x}(t)$ can also be obtained by the inverse Fourier transform of $X_{\mathrm{p}}(\omega)$ as follows:

$$\tilde{x}(t)=\frac{1}{2\pi}\int_{-\infty}^{+\infty}X_{\mathrm{p}}(\omega)\exp(\mathrm{j}\omega t)\mathrm{d}\omega=$$
$$\frac{1}{NT_0}\sum_{n=-\infty}^{\infty}X(n\omega_0)\bullet\exp(\mathrm{j}n\omega_0 t). \tag{13}$$

Although Eq. (13) has an infinite number of terms, the

signal in practice is comprised of finite ones. It is mainly because the terms above Nyquist frequency have already been suppressed by the anti-aliasing filter before sampling. For this reason, Eq. (13) can be rewritten as

$$\tilde{x}(t)=\sum_{k=-L}^{L}\frac{X(k\omega_0)}{NT_0}\exp(\mathrm{j}k\omega_0 t), \tag{14}$$

where $L=\max\{k\,|\,k\omega_0<\omega_s/2\}$, ω_s is the sampling frequency(rad/s). Eq. (14) gives the relationship between CTDA and the discrete samples of $X(\omega)$, which implies that CTDA can be reconstructed as long as $X(k\omega_0)$ is known.

3.2 Estimation of $X(k\omega_0)$ based on chirp Z-transform

In this subsection, how to estimate $X(k\omega_0)$ from the original series $x[n]$ is investigated.

The relationship between discrete-time Fourier transform (DTFT) of $x[n]$ and the Fourier transform of $x(t)$[22] is given by

$$X_{\mathrm{d}}(\omega)=\frac{1}{\Delta t}\sum_{r=-\infty}^{\infty}X\left(\frac{\omega}{\Delta t}-\frac{2\pi n}{\Delta t}\right), \tag{15}$$

where $X_{\mathrm{d}}(\omega)$ is the DTFT of $x[n]$ with length P, which is defined as

$$X_{\mathrm{d}}(\omega)=\sum_{n=-\infty}^{\infty}x[n]\exp(-\mathrm{j}\omega n)=\sum_{n=0}^{P-1}x[n]\exp(-\mathrm{j}\omega n). \tag{16}$$

It is noticed that $X_{\mathrm{d}}(\omega)$ is the frequency normalized periodic extension of $X(\omega)$. When the sampling theorem is satisfied, there is no overlap between the replicas of $X(\omega)$. Hence, $X(k\omega_0)$ can be estimated by the following formula:

$$\begin{aligned}X(k\omega_0)&\approx\Delta tX_{\mathrm{d}}(k\omega_0\Delta t)=\\ &\Delta tX_{\mathrm{d}}(2\pi k\omega_0/\omega_s)=\Delta tX_{\mathrm{d}}(k\Delta\omega).\end{aligned} \tag{17}$$

In fact, $X_{\mathrm{d}}(k\Delta\omega)$, $0\leqslant k\leqslant L$, can be considered as the discrete samples on the unit circle in Z-plane with an angular interval of $\Delta\omega$. Whereas $X_{\mathrm{d}}(k\Delta\omega)$, $-L\leqslant k\leqslant -1$, are points locating symmetrically about real axis with them, which is illustrated in Fig. 3. Now, the remaining problem is how to calculate $X_{\mathrm{d}}(k\Delta\omega)$ with efficiency.

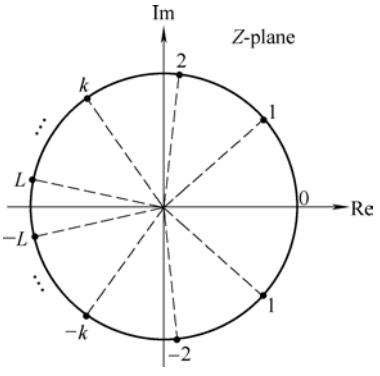

Fig. 3. Sampling points on the unit circle in the proposed TDA

CZT is an effective tool for computing the Z-transform along spiral contours on the Z-plane. For an sequence $x[n]$, its CZT is defined as[23]

$$CZT(x[n])=\sum_{n=0}^{N-1}x[n]\bullet z_k^{-n}=\sum_{n=0}^{N-1}x[n]\bullet(AW^{-k})^{-n}. \tag{18}$$

Unlike the discrete Fourier Transform (DFT), CZT can provide a flexible way to evaluate the Z-transform along contours as illustrated in Fig. 4, which can be described by

$$z_k=A\bullet W^{-k},k=0,\cdots,M-1, \tag{19}$$

where A is the complex starting point, W is a complex scalar specifying the complex ratio between points on the contour, and M is the length of the transform. CZT can be calculated efficiently since the corresponding algorithm is FFT-based. More properties of CZT can be found in Refs. [23–25].

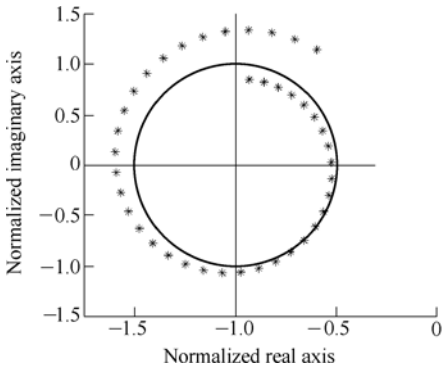

Fig. 4. Illustration of chirp Z-transform on the Z plane

Obviously, $X_{\mathrm{d}}(k\Delta\omega)$, $0\leqslant k\leqslant L$, can be calculated by setting $A=1$, $W=\exp(-\mathrm{j}\Delta\omega)$, $M=L+1$ in Eq. (18). The remaining values can be obtained immediately since they are complex conjugate with the former ones.

Substituting those values into Eq. (14), we have

$$\begin{aligned}\tilde{x}(t)&=\sum_{k=-L}^{L}\frac{\Delta tX_{\mathrm{d}}(k\Delta\omega)}{NT_0}\exp(\mathrm{j}k\omega_0 t)=\\ &\sum_{k=-L}^{L}c_k\exp(\mathrm{j}k\omega_0 t)=a_0+\sum_{k=1}^{L}a_k\cos(k\omega_0 t+\varphi_k).\end{aligned} \tag{20}$$

where a_0, a_k, φ_k are the DC component, amplitude and initial phase of the kth harmonic of TDA, respectively.

Eq. (20) gives the harmonic information of the periodic signal we are interested in an explicit way. Discrete TDA can be obtained by discretizing Eq. (20) with a proper resampling frequency, say f_{ns}. For instance, when $f_{\mathrm{ns}}=f_{\mathrm{s}}$, it has the same sampling interval as conventional one. When we choose $f_{\mathrm{ns}}>f_{\mathrm{s}}$, a smoother waveform of TDA can be obtained, which is equivalent to an interpolation form of the conventional TDA. At the same time, signal de-noising

can be achieved by eliminating a_ks whose magnitudes fall below the threshold according to some criterions. We can also extract some certain harmonics by retaining the corresponding a_ks.

Although the derivation of FTDA is cumbersome, its implementation is very convenient, which can be summarized as follows:

Step 1. Determine the fundamental frequency (ω_0) of the interested periodic components.

Step 2. Calculate the Fourier series coefficients c_k in Eq. (20) from the original data $x[n]$ based on CZT;

Step 3. Achieve signal de-noising or filtering by setting the corresponding coefficients to zero;

Step 4. Obtain the discrete TDA by sampling Eq. (20) with an appropriate sampling frequency according to one's need.

4 Numerical Simulation

A numerical simulation is presented to testify the efficiency of the FTDA. The direct TDA and an improved TDA[15] are also applied to process the same simulated data for comparisons, which are defined as DTDA and ITDA, respectively.

The simulated signal is composed of three components, which is given as

$$X(t)=X_{\mathrm{p}}(t)+X_{\mathrm{n}}(t)+w(t)=\sum_{k=1}^{K}A_k\cos(2\pi kf_0+\alpha_k)+\sum_{l=1}^{L}B_l\cos(2\pi lf_1+\beta_l)+w(t). \tag{21}$$

where $X_{\mathrm{p}}(t)$ is the periodic component we want to extract; $X_{\mathrm{n}}(t)$ represents the asynchronous periodic interferences generated by other rotating components; $w(t)$ is the zero mean white noise. The fundamental frequency of $X_{\mathrm{p}}(t)$ and $X_{\mathrm{n}}(t)$ are $f_0=116$ Hz and $f_1=109$ Hz, respectively. The sampling frequency f_{s} is 2 000 Hz, and the data length is 2 000. Other parameters in Eq. (21) are listed in Table 1.

Table 1. Parameter selection in the simulation

Amplitude A_k/g ($k=1, 2, 3, 4$)	Phase α_k/rad ($k=1, 2, 3, 4$)	Amplitude B_l/g ($l=1, 2, 3, 4$)	Phase β_l/rad ($l=1, 2, 3, 4$)
1	$\pi/6$	1.5	$\pi/6$

The SNR of $X(t)$ is –5 dB. The waveform and spectrum of $X(t)$ are illustrated in Fig. 5. It can be seen that the periodic signal $X_{\mathrm{p}}(t)$ is corrupted significantly in both time and frequency domain.

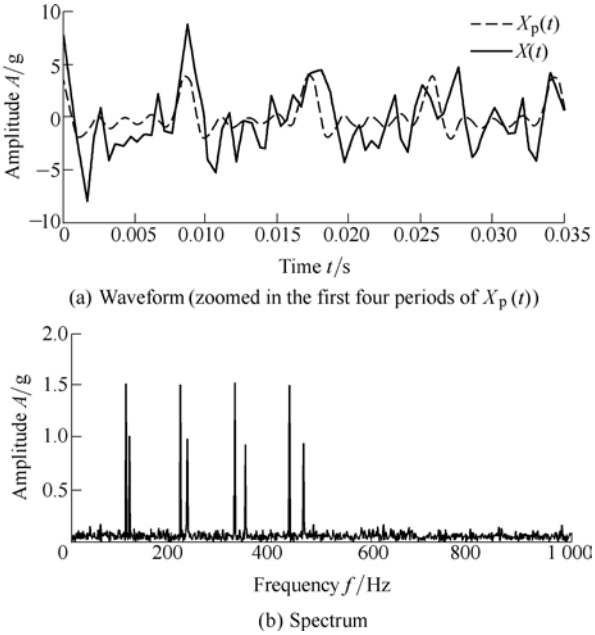

Fig. 5. Waveform and spectrum of simulated signal

DTDA, ITDA and FTDA are applied to the simulated signal respectively for comparisons. The number of the periods for averaging is 100.

The result obtained by DTDA is given in Fig.6(a). Apparently, there is a significant deviation from $X_{\mathrm{p}}(t)$, the SNR of the result is only –0.4 dB. In this case, the attenuation coefficients C_k, for $k=1, 2, 3, 4$, is only 0.216, 0.067, 0.045, 0.054, respectively. It reveals why the performance of DTDA is not good. The result obtained by ITDA is shown in Fig.6(b). The performance is much better than DTDA, the SNR attains 14.5 dB. However, the detail information of the waveform is missing due to its poor time resolution of the algorithm.

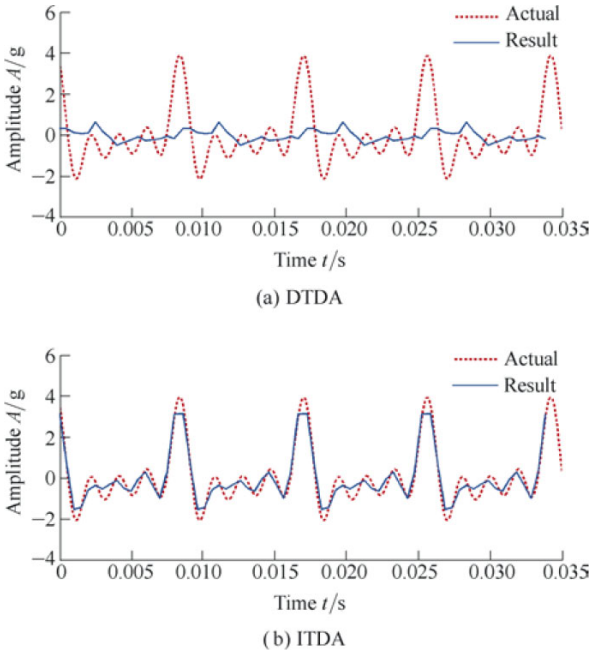

Fig. 6. Results of conventional TDA

The resampling frequency f_{ns} can be selected flexibly in the FTDA. In order to have a clear description of the periodic signal, we choose $f_{ns} = 10f_s$ in FTDA. The corresponding result is shown in Fig. 7(a). Detail information is recovered completely, and the SNR is improved to 22.4 dB in this case.

At the same time, the FTDA can also be used for signal de-noising. For instance, if the threshold is taken 0.2, all the coefficients below threshold are forced to zero, then the SNR of the result will attain 38.2 dB, which is shown in Fig. 7(b). Moreover, the outputs of DTDA and ITDA are the total contributions of fundamental frequency and its all harmonics, therefore we cannot figure out the contribution of specified harmonics. As discussed in section 3, this constrain of conventional TDA can be overcome by retaining only the harmonics of interest before sampling in the proposed approach. Fig. 8(a) and Fig. 8(b) illustrate the extracted waveform of fundamental frequency and its 2–4th harmonics, respectively. It is noticed that both of them are consistent well with the actual ones. In fact, signal filtering can also be performed in a similar way.

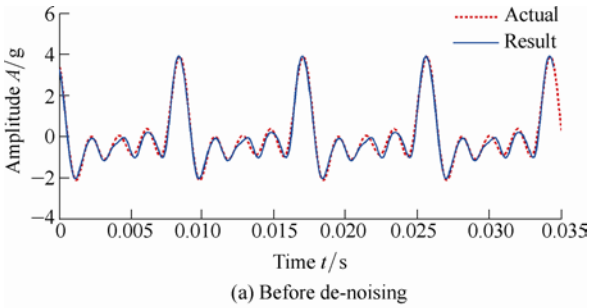

Fig. 7. Result of FTDA

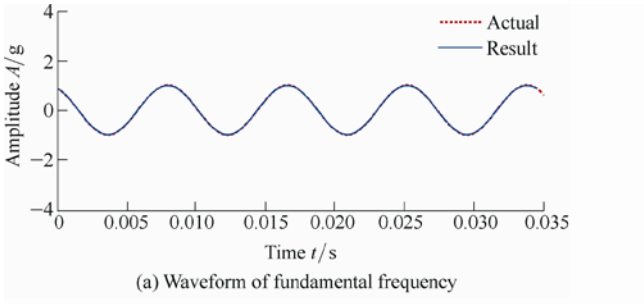

Fig. 8. Harmonics extraction using FTDA

5 Experimental Verification

In this section, FTDA is applied to detect fault for gearboxes to demonstrate the efficiency.

Example 1. Tooth damage detection

The test rig consists of three shafts and two pairs of meshing gears. The tooth number of each gear is given in Fig. 9.

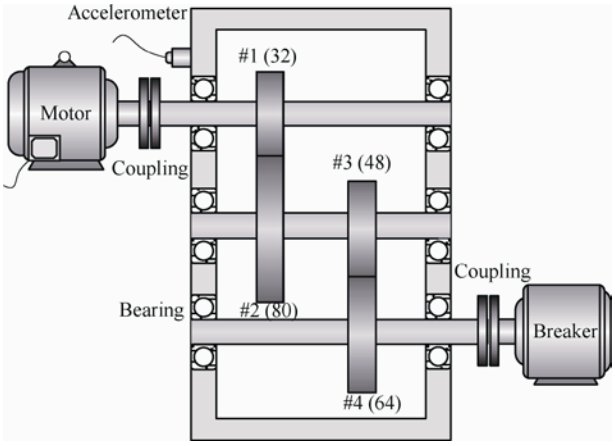

Fig. 9. Experimental setup

The rotating frequency of the input shaft is 10 Hz during the experiment. Therefore, the rotating frequency of the idler shaft and that of the output shaft are 4 Hz and 3 Hz respectively. Accordingly, the meshing frequencies are 320 Hz and 192 Hz respectively. The vibration signal is acquired by mounting an accelerometer on the bearing cap of the input shaft. The sampling frequency is 4 000 Hz. Spur gears are used in the test rig. The damage is generated by chipping off a piece on Gear #1, as is shown in Fig. 10 .

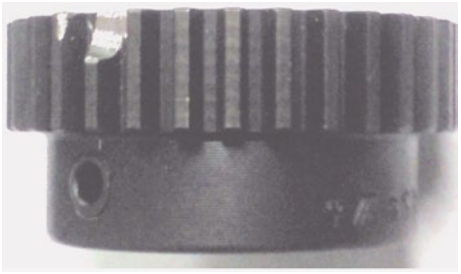

Fig. 10. Faulty gear used in the experiment.

The vibration signal is shown in Fig. 11, from which we fail to find clear indications of the damage. In order to capture the signature of the damage, three TDA algorithms are applied to process the vibration signal and the results are shown in Fig. 12. The number of segments for averaging is 80.

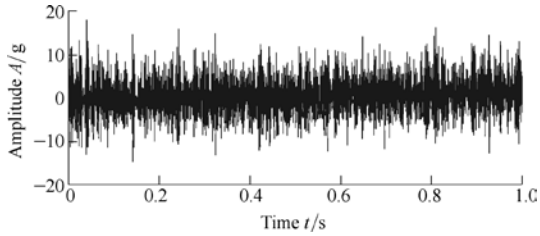

Fig. 11. Waveform of vibration signal

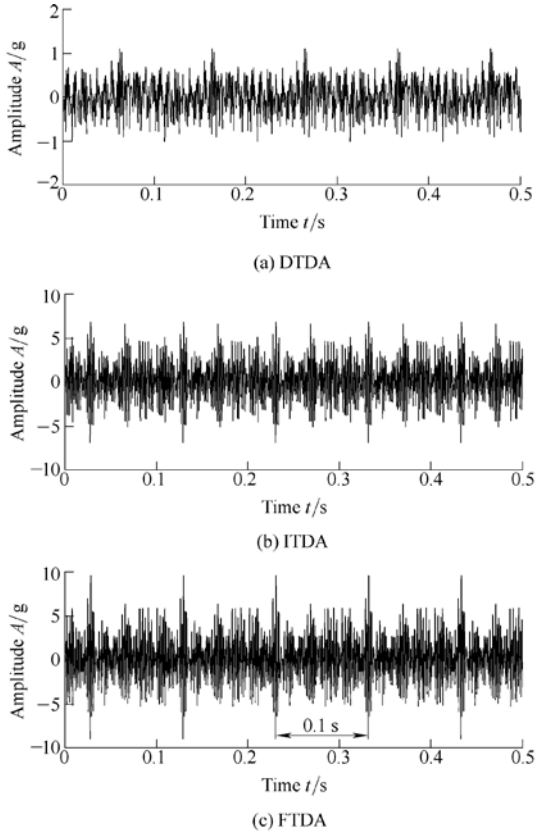

Fig. 12. Result of three TDA algorithms

The result by DTDA is shown in Fig. 12(a). Periodic impulses generated by the damage gear cannot be observed clearly. Fig. 12(b) shows the result by ITDA, the periodic impulses are not clear as well. The result by FTDA is shown in Fig. 12(c), form which we can easily find the impulses introduced by fault with an interval of 0.1s. It is also noticed that the amplitudes of those impulses are enhanced by 35% compared with ITDA.

Example 2. Gear eccentricity identification

Gear eccentricity is a typical fault encountered frequently in practice. In this example, we will illustrate how to identify it by using FTDA.

The vibration signal in this example is provided by the 2009 PHM Challenge Competition, which is measured on a gearbox with the same structure as shown in Fig. 9. The tooth numbers of each gear are 32, 96, 48, 80, respectively. The rotating frequency of the input shaft is 34.5 Hz during the measurement and the sampling frequency is 66.67 kHz. Gear #3 is the fault gear with eccentricity.

The waveform of the vibration signal is shown in Fig. 13, from which we could not find obvious signature such as periodic amplitude modulated components. The result by ITDA is given in Fig. 14(a). Some periodic components due to eccentricity can be found. However, we cannot figure out the severity and direction of the eccentricity. The main reason for this phenomenon can be stated as follows. The eccentric fault is characterized by the first sidebands around the meshing frequency due to amplitude modulation. However, the output of the ITDA contains all the harmonics, which may lead low SNR to the output. This deficiency can be overcome by using FTDA because we can choose specified harmonics flexibly. The output waveform of the proposed method with a retaining of 47–49th harmonics of rotating frequency is illustrated in Fig. 14(b). The amplitude modulation caused by eccentric gear is clearly identified. Meanwhile, the severity and direction of the eccentricity can also be determined according to the amplitudes and angular positions of those peaks. The result corresponding to healthy gear is also given in Fig. 15 for comparison. No obvious amplitude modulation can be seen in that figure.

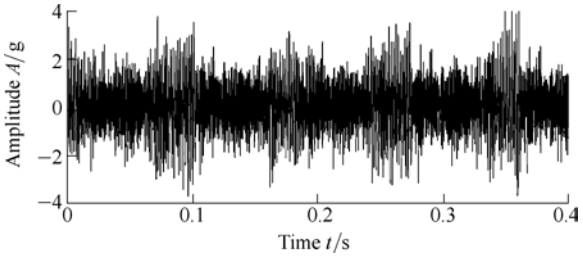

Fig. 13. Waveform of the vibration signal

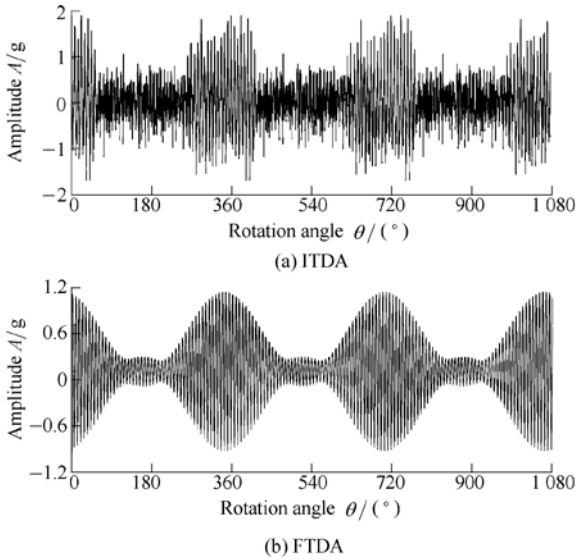

Fig. 14. Amplitude modulation of eccentric gear

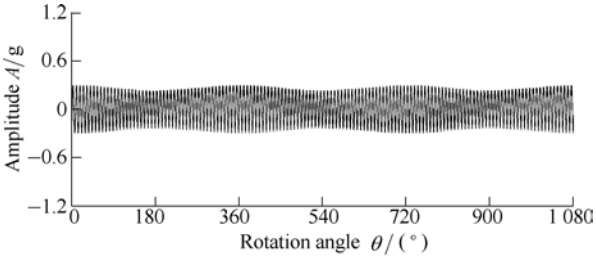

Fig. 15. Amplitude modulation of healthy gear

6 Conclusions

(1) The attenuation coefficient of TDA is derived, with which, the performance of TDA methods can be assessed quantitatively.

(2) The relationship between continuous TDA and frequency domain sampling is investigated. It can be concluded that the period cutting error encountered in the conventional approaches can be eliminated effectively by chirp Z-transform in an implicit way.

(3) The advantage of the proposed FTDA is that it not only achieves the same de-noising effect as conventional ones, but also could be used in order extraction and interpolation.

(4) The fault signatures of a gearbox such as chipped tooth and gear eccentricity are effectively captured by the proposed technique.

References

[1] MOHANTY A R, KAR C. Fault detection in a multistage gearbox by demodulation of motor current waveform[J]. *IEEE Transactions on Industrial Electronics*, 2006, 53(4): 1 285–1 297.

[2] JARDINE A K S, LIN Daming, BANJEVIC D. A review on machinery diagnostics and prognostics implementing condition-based maintenance[J]. *Mechanical Systems and Signal P rocessing*, 2006, 20(7): 1 483–1 510.

[3] RANDALL R B, ANTONI J. Rolling element bearing diagnostics—A tutorial[J]. *Mechanical Systems and Signal Processing*, 2011, 25(2): 485–520.

[4] ZHANG Xiaofei, HU Niaoqing, CHENG Zhe, et al. Enhanced detection of rolling element bearing fault based on stochastic resonance[J]. *Chinese Journal of Mechanical Engineering*, 2012, 25(6): 1 287–1 297.

[5] FENG Zhipeng, ZUO Mingjian. Vibration signal models for fault diagnosis of planetary gearboxes[J]. *Journal of Sound and Vibration*, 2012, 331(22): 4 919–4 939.

[6] CHENG Zhe, HU Niaoqing. Quantitative damage detection for planetary gear sets based on physical models[J]. *Chinese Journal of Mechanical Engineering*, 2012, 25(1): 190–196.

[7] BRAUN S. The extraction of periodic waveforms by time domain averaging[J]. *Acustica*, 1975, 32(2): 69–77.

[8] MCFADDEN P D. A revised model for the extraction of periodic waveforms by time domain averaging[J]. *Mechanical Systems and Signal Processing*, 1987, 1(1): 83–95.

[9] MCFADDEN P D, TOOZHY M M. Application of synchronous averaging to vibration monitoring of rolling element bearings[J]. *Mechanical Systems and Signal Processing*, 2000, 14(6): 891–906.

[10] HALIM E B, CHOUDHURY M A A S, SHAH S L, et al. Time domain averaging across all scales: A novel method for detection of gearbox faults[J]. *Mechanical Systems and Signal Processing*, 2008, 22(2): 261–278.

[11] ZHU Limin, HE Enhua, DING Han. Comb filter array and its application[J]. *Journal of Mechanical Engineering*, 2006, 42(5): 1–5. (in Chinese)

[12] MCFADDEN P D. A technique for calculating the time domain averages of the vibration of the individual planet gears and the sun gear in an epicyclic gearbox[J]. *Journal of Sound and Vibration*, 1991, 144(1): 163–172.

[13] SHIN K. Realization of the real–time time domain averaging method using the Kalman filter[J]. *International Journal of Precision Engineering and Manufacturing*, 2011, 12(3): 413–418.

[14] YANG Ming, MAKIS V. ARX model–based gearbox fault detection and localization under varying load conditions[J]. *Journal of Sound and Vibration*, 2010, 329(24): 5 209–5 221.

[15] LIU Hongxing, ZUO Hongfu, JIANG Chengyu, et al. An improved algorithm for direct time–domain averaging[J]. *Mechanical Systems and Signal Processing*, 2000, 14(2): 279–285.

[16] MCFADDEN P D. Interpolation techniques for time domain averaging of gear vibration[J]. *Mechanical Systems and Signal Processing*, 1989, 3(1): 87–97.

[17] WU Wentao, LIN Jing, HAN Shaobo, et al. Time domain averaging based on fractional delay filter[J]. *Mechanical Systems and Signal Processing*, 2009, 23(5): 1 447–1 457.

[18] BRAUN S. The synchronous(time domain) average revisited[J]. *Mechanical Systems and Signal Processing*, 2011, 25(4): 1 087–1 102.

[19] EBRAHIMI E. Fault diagnosis of spur gear using vibration analysis[J]. *Journal of American Science*, 2012, 8(1): 133–138.

[20] SAMUEL P D, PINES D J. A review of vibration-based techniques for helicopter transmission diagnostics[J]. *Journal of Sound and Vibration*, 2005, 282(1): 475–508.

[21] WANG Xiyang, Makis V, YANG Ming. A wavelet approach to fault diagnosis of a gearbox under varying load conditions[J]. *Journal of Sound and Vibration*, 2010, 329(9): 1 570–1 585.

[22] OPPENHEIM A V, SCHAFER R W, BUCK J R. *Discrete-time signal processing*[M]. New Jersey: Prentice Hall, 1999.

[23] RABINER L, SCHAFER R, RADER C. The chirp z-transform algorithm[J]. *IEEE Transactions on Audio and Electroacoustics*, 1969, 17(2): 86–92.

[24] WANG T T. The segmented chirp Z-transform and its application in spectrum analysis[J]. *IEEE Transactions on Instrumentation and Measurement*, 1990, 39(2): 318–323.

[25] SARKAR I, FAM A T. The interlaced chirp Z transform[J]. *Signal Processing*, 2006, 86(9): 2 221–2 232.

Biographical notes

ZHAO Ming is currently a doctoral candidate at *School of Mechanical Engineering*, *Xi'an Jiaotong University*, *China*. He received his BS and MS degrees from *Xi'an Jiaotong University*, *China*, in 2006 and 2009, respectively. His research interests include non-stationary signal processing, rotor dynamics and fault diagnosis of rotating machinery.

Tel: +86-29-83395041; E-mail: zhao_ming@stu.xjtu.edu.cn

LIN Jing is a professor at *State Key Laboratory for Manufacturing System Engineering, Xi'an Jiaotong University*, *China* He obtained his BSc, MSc and PhD degrees respectively in 1993, 1996 and 1999, all in mechanical engineering. He was working as a postdoctoral fellow and research associate from July 2001 to August 2003, respectively in *University of Alberta, Canada*, and *University of Wisconsin-Milwaukee*, *USA*. From September 2003 to December 2008, he was working as a research scientist at *Institute of Acoustics, Chinese Academy of Sciences*, under the sponsorship of the Hundred Talents Program. He also obtained the National Science Fund for Distinguished Young Scholars in 2011. Now his research directions are non-stationary signal processing, wavelet analysis, fault diagnosis and mechanical system reliability.

Tel: +86-29-83395041; E-mail: jinling@mail.xjtu.edu.cn

LEI Yaguo received his bachelor degree in 2002 and PhD degree in 2007 both in mechanical engineering from *Xi'an Jiaotong University, China*, and worked as a postdoctoral fellow at *Department of Mechanical Engineering, University of Alberta, Canada*. He is currently an associate professor in mechanical engineering of *Xi'an Jiaotong University, China*. His research interests include advanced signal processing techniques, hybrid intelligent prognostics and machinery health condition monitoring and fault diagnosis.
Tel: +86-29-83395041; E-mail: yaguolei@mail.xjtu.edu.cn

WANG Xiufeng received his BS and PhD degrees from *Xi'an Jiaotong University* in 2003 and 2009, respectively. He is currently a lecturer in mechanical engineering of *Xi'an Jiaotong University, China*. His research interests include rotor dynamics and vibration control.
Tel: +86-29-83395041; E-mail: wangxiufeng@mail.xjtu.edu.cn